

Existence of a tricritical point at finite field in the three-dimensional random-field Ising model

Laura Hernández* and H. T. Diep

Groupe de Physique Statistique, Université de Cergy-Pontoise, 2, Avenue Adolphe Chauvin, 95302 Cergy-Pontoise Cedex, France

(Received 16 October 1996)

The critical behavior of the random-field Ising model with a bimodal field distribution is studied using standard and histogram Monte Carlo calculations. It is definitely found that the transition is second order for weak fields while it becomes first order for higher fields. The existence of this crossover, discovered here in Monte Carlo simulations, is in contradiction with earlier Monte Carlo works, but in agreement with mean-field predictions. Estimates of the critical exponents of the model at low field are given. [S0163-1829(97)01722-0]

I. INTRODUCTION

In spite of much theoretical and experimental effort done to understand the random-field Ising model (RFIM), several aspects remain unclear. After the works of Imry and Ma¹ and Imbrie,² its lower critical dimension is now well established to be $d_l=2$. On the contrary, the nature of the transition for $d>2$ is not yet clarified. Though mean-field results³ indicate the existence of a tricritical point (TCP) at sufficiently high fields for the bimodal distribution, standard Monte Carlo (MC) calculations in $d=3$, performed assuming a second-order transition,^{4,5} give $\beta\sim 0$, suggesting a first-order transition or an extremely sharp second-order one for any finite field. Exact ground-state calculations at the zero fixed point also suggest a weak first-order transition for the bimodal distribution.⁶ Even when the transition is assumed to be second order, estimates of critical exponents issued from analytical and numerical works are not coincident^{4,5,7,8} and depend on the intensity of the random field. The nature of the ordered phase at low temperatures is also poorly understood. Furthermore, suitable scenarios to understand the critical behavior are under discussion. The droplet picture indicates a modification of hyperscaling via a third independent exponent θ which controls the extremely long relaxation times.¹⁰⁻¹² On the other hand, a new high-temperature series expansion suggests the existence of a new scaling relationship between the exponents governing the critical behavior of the susceptibility and that of the disconnected susceptibility, leaving only two independent critical exponents,^{8,9} in contradiction to the droplet picture.

In this article we address our study to the question of the nature of the transition in the RFIM with a bimodal field distribution, using standard and histogram MC (SMC and HMC, respectively) calculations.¹³ The histogram method allows us to map the probability distribution in the critical region and to obtain the critical exponents via finite size scaling (FSS). As shown below, we clearly find a crossover between a second- and first-order behavior *at a finite value of the field intensity*.

In Sec. II we describe the model and calculation techniques used here, in Sec. III we give our results, and in Sec. IV we discuss our results and give a conclusion.

II. MODEL AND CALCULATION TECHNIQUES

We have considered the following Hamiltonian on a simple cubic lattice of linear dimension L :

$$H = -J \sum_{\langle i,j \rangle} s_i s_j - g \mu_B \sum_i H_i s_i, \quad (1)$$

where $s_i = \pm 1$, the first sum being performed over the nearest-neighbor (NN) pairs. H is the quenched random field intensity, J is the ferromagnetic interaction constant between NN's, g the gyromagnetic factor, and μ_B the Bohr magneton. We define $h = g \mu_B H / k_B$; then the field distribution is written as

$$P(h_i) = \frac{1}{2} [\delta(h_i - h) + \delta(h_i + h)], \quad (2)$$

where h_i is the field at site i .

In the following we use $J/k_B = 1$; the temperature and magnetic field h will be given in units of J/k_B .

We have studied systems of $L=16,20,24,30,36,40$ with periodic boundary conditions. As a first step we have performed SMC field heating (FH) and field cooling (FC) calculations for different field intensities ($h = 0.5, 1, 1.5, 1.9, 2, 2.1, 2.2$). These calculations help us to (a) classify the (T, h) plane in two regions: low field and high temperature, where we expect the transition to be continuous, and high field and low temperature, where the transition might be first order, and (b) get an estimate of the transition temperature $T_0(L)$ corresponding to each value of h that will then be used as an input of the HMC calculations.

We have then performed HMC calculations at T_0 for each lattice size. We also studied different quenched field configurations for $h=0.5$ where the SMC results indicate a second-order transition. SMC results show that the transition is second order up to, at least, $h=1$, and so the estimates of the critical exponents calculated at $h=0.5$ should not be affected by the existence of a TCP. We have also performed some runs to map the probability distribution at higher values of the field, where SMC calculations suggests a first-order behavior.

We can test the equilibration of the system by monitoring the magnetization and the energy as functions of MC time. We have found that equilibrium is easily achieved for low fields but is harder to obtain as the intensity of the random field increases. The length of each run varies as a function of L . Typically, for the HMC calculations, we have used 10^6 Monte Carlo steps per second (MCS/s) for thermalization and 2×10^6 MCS/s for averaging for the largest lattices.

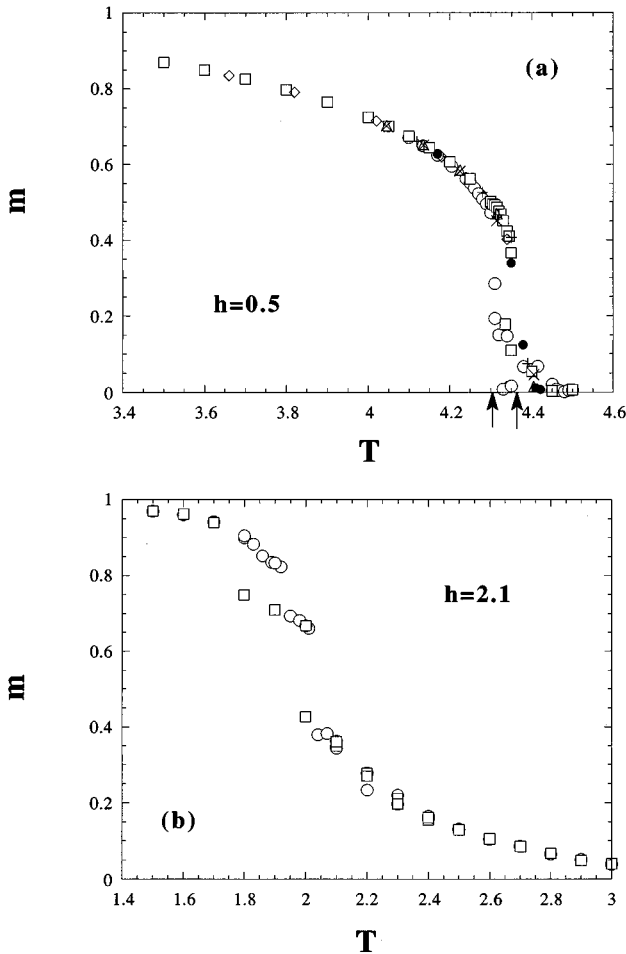


FIG. 1. Magnetization as a function of temperature $m(T)$ is shown for two values of h : (a) $h=0.5$, (\circ) $L=20$, (\square) $L=24$, (\triangle) $L=24$, (\diamond) $L=30$, (\times) $L=30$, ($+$) $L=36$, and (\bullet) $L=40$ (results issued from two different quenched field configurations are included for $L=24,30$). The arrows indicate the location of extreme T_0 values, observed for $L=20$ and $L=40$. The shift due to sample to sample fluctuations is even smaller, and so two different samples will have different $T_c(L)$ but the same critical region within less than 2%. The continuous aspect of the curves should be compared to that of (b). (b) $h=2.1$, (\circ) FH, and (\square) FC for $L=24$. Jumps, metastable states, and hysteresis are clearly observed, suggesting that the transition is first order.

III. RESULTS

Figure 1, issued from SMC calculations, shows the difference in the magnetization curves as a function of temperature for two values of the field. Curves in Fig. 1(a), corresponding to $h=0.5$, look continuous and this characteristic remains when increasing the lattice size. It can be observed that T_0 depends not only on L but also on different configurations of quenched disorder. Combining these two factors, we can define a region limited by the extreme observed values of T_0 . The width of this region, which will give the temperature input value for the HMC, is about 2% of the mean T_0 and is expected to decrease with increasing L . This indicates that the lattice sizes we are working with are large enough to exclude the possibility that the continuous aspect of the transition is a finite-size effect. $m(T)$ curves for two distributions of quenched disorder are also displayed in Fig. 1(a) for

$L=24,30$, showing only a slight shift of T_0 . We believe that this relatively small shift observed for T_0 at a given L is due to the *zero-total-field* constraint that we imposed on the system, contrary to previous works.^{4,5} We will see later that this shift, which may be considered small for the required precision of T_0 , becomes important when performing the FSS to determine $T_c(\infty)$ necessary to calculate the exponent β .

On the other hand, in Fig. 1(b), we show a magnetization FH-FC loop for $L=24$, $h=2.1$. The shape of the $m(T)$ curves is clearly different from those in Fig. 1(a). We can observe that FH and FC curves are coincident for high and low T (long-range order is achieved in FC), leaving a zone in between which shows hysteresis along with jumps and metastable states, suggesting that the transition might be first order.

Energy distributions, issued from HMC calculations at T_0 , are shown in Fig. 2. At *low but finite* field, the critical region has been carefully explored (by changing T_0) and only a large single peak has been found. In Fig. 2(a) *two* histograms obtained at the same T_0 , but issued from initial random and ferromagnetic configurations, are shown. The fact that both collapse on the same single-peaked distribution is an additional proof of the second-order nature of the transition—i.e., no hysteresis is observed—and also indicates that equilibrium is reached.

On the other hand, a double-peak distribution is observed at higher fields [see Fig. 2(b)], clearly indicating that the transition is first order. However, due to the hysteresis effect, which is characteristic of a first-order transition, the resulting structure of the histogram depends on the initial configuration of the system, as is also shown in Fig. 2(b): The single-peaked histogram is obtained at the same temperature when the simulation starts from a ferromagnetically ordered configuration. This result can be schematically described by the inset of Fig. 2(b): If the transition is first order, two histograms calculated at the same T_0 , but starting from different initial states, follow a different path in the state space. When the initial configuration is ferromagnetic, the system follows a path that leads it to a state represented by point A in the inset of Fig. 2(b). This state is stable for the path in the space state the system has followed, and so we find only one peak in the histogram.

On the other hand, when the initial configuration is random the followed path will first lead the system to point B at T_0 , where the histogram is measured. The system becomes unstable for the followed path, and so it also visits state A. In this case we observe a two-peak histogram. The energy as a function of time curve fluctuates between the two values corresponding to the peaks of the distribution. This is clearly a characteristic of a first-order transition, and not a nonequilibrium effect.

From the above results, we conclude that there exists a tricritical point at some particular value of T and h where a crossover between second- and first-order behavior takes place.

This is in contradiction to Young and Nauenberg⁴ who suggested that the transition should be first order for all finite values of field based on the fact that the γ and η they calculated using SMC calculations and assuming second-order transition do not verify the Schwartz inequality.

We have performed a preliminary calculation of the criti-

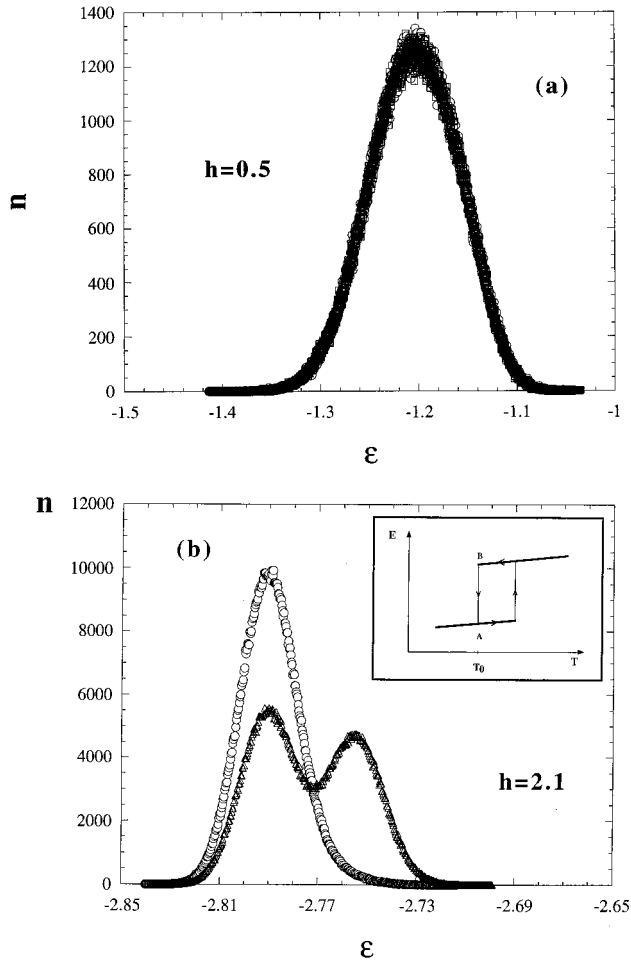


FIG. 2. (a) Probability distribution (number of configurations, n), as a function of the energy per spin, ϵ) for $h=0.5$, $L=30$. No double-peak structure has been found in the critical region. Two histograms issued from two simulations performed at the same T_0 but starting from ferromagnetic and random initial conditions, respectively, collapse on the same single peaked distribution. (b) The same for $h=2.1$, $L=24$; the two-peak structure is obtained when the initial configuration is random, and the single-peaked histogram is issued from a ferromagnetically ordered initial crystal at the same T_0 . The inset shows schematically a FH-FC loop. The energies of the peaks correspond to those of points A and B of the inset (see text for detailed explanation).

cal exponents in the low-field region in order to test whether the system follows second-order FSS laws. We have then calculated

$$V_{1\max}(L) \propto L^{1/\nu}, \quad (3)$$

$$V_{2\max}(L) \propto L^{1/\nu}, \quad (4)$$

where

$$V_1(T) = \frac{\partial \langle m \rangle}{\partial \beta} = \langle mE \rangle - \langle m \rangle \langle E \rangle, \quad (5)$$

$$V_2(T) = \frac{\partial \langle m^2 \rangle}{\partial \beta} = \langle m^2 E \rangle - \langle m^2 \rangle \langle E \rangle. \quad (6)$$

E is the energy of the system and $\beta = 1/k_B T$.

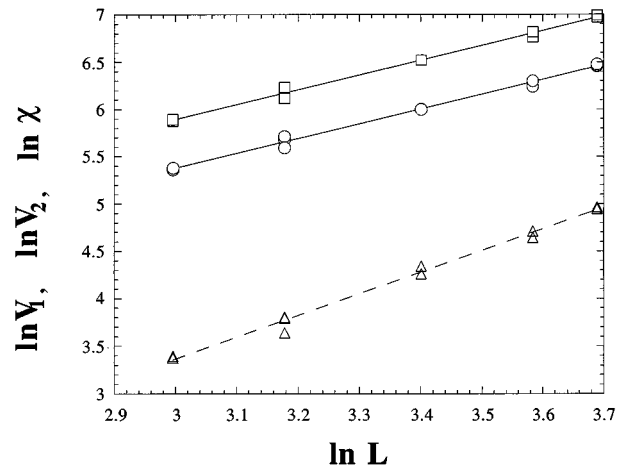


FIG. 3. Preliminary FSS calculation of critical exponents ν and γ . (○) ν from Eq. (3), (□) ν from Eq. (4), and (△) γ from Eq. (7). The straight line corresponds to the linear fit. Different points for a given lattice correspond to different quenched disorder configurations.

In Fig. 3 we show the FSS calculation of ν issued from Eqs. (3) and (4) and that of γ issued from the fit of the log-log plot of the susceptibility maximum as a function of L :

$$\chi_{\max}(L) \propto L^{\gamma/\nu}. \quad (7)$$

Equations (3) and (4) give two estimates of ν . Its final value is then calculated as the mean value of the two, giving $\nu = 0.64 \pm 0.015$. The value obtained for the susceptibility critical exponent is $\gamma = 1.46 \pm 0.07$.

According to the Harris criterion,¹⁴ one expects the pure 3d Ising exponents to be modified by the presence of disorder induced by the random field. This is indeed the case: The values of the critical exponents obtained from Fig. 3 are different from those of the pure 3d Ising case¹³ ($\nu_I = 0.6289 \pm 0.0008$, $\gamma_I = 1.2390 \pm 0.071$, $\beta_I = 0.3258 \pm 0.0044$).

We are not able to obtain an estimate for β at this stage. This is due to the fact that to calculate β we need the critical temperature of the infinite system $T_c(\infty)$ which is usually obtained by extrapolating the $T_c(L)$ values given by the peaks' positions of the different calculated quantities [$\chi(T)$, $V_1(T)$, $V_2(T)$, etc.]. We have observed that sample-to-sample fluctuations are more important in the precise location of $T_c(L)$ than in the value of the peak itself (see Fig. 3). Then, a good estimate of $T_c(\infty)$ is very difficult to obtain.

Now, it is worthwhile to make two remarks. First, the suggestion of Refs. 4 and 5 that the transition at low fields is first order would imply that the transition at the zero-field limit is a tricritical point: We know that it is not true. So we believe that the second-order transition is more plausible. Second, the critical exponents estimated above verify well the FSS laws as seen in Fig. 3. This excludes the possibility of the transition being first order since, in this case, the response functions scale as the volume of the system.¹⁵ The fact of obtaining a slope smaller than 3 in Fig. 3, where $\gamma/\nu = 2.28 \pm 0.06$, is a clear indication of that the transition is not first order for this value of the field.

IV. DISCUSSION AND CONCLUSION

Our results clearly show that the RFIM with a bimodal distribution has a TCP at finite T and h . This is consistent with mean-field (MF) and renormalization-group (RG) results,^{3,16} which indicate that, if the probability distribution has a minimum at the origin, then a TCP exists at sufficiently low T . The MF phase diagram given by Aharony³ in four dimensions surprisingly applies to the Ising in three dimensions studied here: At high fields, the transition is first order and it becomes second order at low fields.

On the other hand, our result is in contradiction with previous SMC calculations,⁴ which suggested the transition to be first order for all finite values of h . We believe that this suggestion is not plausible as discussed above.

Let us compare now our preliminary values of critical exponents to those found by Rieger and Young⁵ using SMC calculations. The difference may lie on different grounds. First, they have assumed that no TCP occurs along the critical line (T_c, h_c) and then that the critical exponents will be the same on that line. We believe that their numerical values for the exponents (which vary as a function of the ratio h/T within a considerable error) may be affected by the vicinity of the crossover to first-order behavior as the values of the field they have chosen are equivalent to taking $h \sim 1, 1.2, \text{ and } 1.5$. The possibility of having the values of the critical exponents affected by the vicinity of a TCP has been suggested by high series expansion calculations.^{8,9}

Second, they have considered very small lattice sizes (up to $L=16$) and used SMC calculations. In this case, corrections to scaling and to FSS may be considerable. In our case the low value of the field allows us to equilibrate large enough lattice sizes so as to avoid, in a first approach, corrections to FSS as discussed above. On the other hand, HMC

simulations allow us to obtain all the necessary quantities as *continuous* functions of the temperature from long runs in the critical region, and so no interpolation to determine the peak of response functions is needed. Finally, Rieger and Young⁵ did not impose the zero-total-field condition. This condition was supposed to be obtained in their calculation by averaging over many different configurations. In our case, we imposed this zero total field which assures that *each sample* has a phase transition. This also reduces fluctuations from sample to sample as shown in Fig. 1(a).

It is worthwhile to notice that the problem of calculating critical exponents of the RFIM is far from being solved. Our preliminary values of γ agree with those given in Refs. 17 and 18 ($\gamma=1.42-1.48$ and $\gamma=1.58-1.6$, respectively). However, there is a large spread of numerical values in the literature. We believe that one of the most important sources of disagreement comes from the fact of neglecting the existence of a TCP. In the other limit, it is also possible that, due to the small value of the field ($h=0.5$), our values are affected by the vicinity of the Ising fixed point. So further calculations of the exponents at different values of h are necessary.

In conclusion, let us emphasize that we have found evidence of the existence of a TCP on the (T_c, h_c) line. This numerical simulation agrees with the MF and RG predictions, unlike early MC works. We believe that further calculations of critical exponents by multihistogram techniques with many quenched field distributions at different *low-field* values and with *large enough lattices* would be necessary to determine if there is a RFIM universality class.

ACKNOWLEDGMENT

The authors are grateful to H. Orland for enlightening discussions.

*Electronic address: laura@u-cergy.fr

¹Yoseph Imry and Shang-keng Ma, Phys. Rev. Lett. **35**, 1399 (1975).

²John Z. Imbrie, Phys. Rev. Lett. **53**, 1747 (1984).

³Amnon Aharony, Phys. Rev. B **18**, 3318 (1978); **18**, 3328 (1978).

⁴A. P. Young and M. Nauenberg, Phys. Rev. Lett. **54**, 2429 (1985).

⁵Heiko Rieger and A. Peter Young, J. Phys. A **26**, 5279 (1993).

⁶Andrew T. Ogielski, Phys. Rev. Lett. **57**, 1251 (1986).

⁷Alexis Falicov, A. Nihat Berker, and Susan R. McKay, Phys. Rev. B **51**, 8226 (1995).

⁸Michael Gofman, Joan Adler, Amnon Aharony, A. B. Harris, and Moshe Schwartz, Phys. Rev. Lett. **71**, 1569 (1993), and references therein.

⁹Misha Gofman, Joan Adler, Amnon Aharony, A. B. Harris, and Moshe Schwartz, Phys. Rev. B **53**, 6362 (1996).

¹⁰Daniel S. Fisher, Phys. Rev. Lett. **56**, 416 (1986).

¹¹A. J. Bray and M. A. Moore, J. Phys. C **18**, L927 (1985).

¹²J. Villain, J. Phys. (Paris) **46**, 1843 (1985).

¹³Alan Ferrenberg and D. P. Landau, Phys. Rev. B **44**, 5081 (1991), and references therein.

¹⁴A. B. Harris, J. Phys. C **7**, 1761 (1974).

¹⁵Murty S. S. Challa, D. P. Landau, and K. Binder, Phys. Rev. B **34**, 1841 (1986).

¹⁶David Andelman, Phys. Rev. B **27**, 3079 (1983).

¹⁷A. Houghton, A. Khurana, and F. J. Seco, Phys. Rev. B **34**, 1700 (1986).

¹⁸H. E. Cheung, Phys. Rev. B **33**, 6191 (1986).